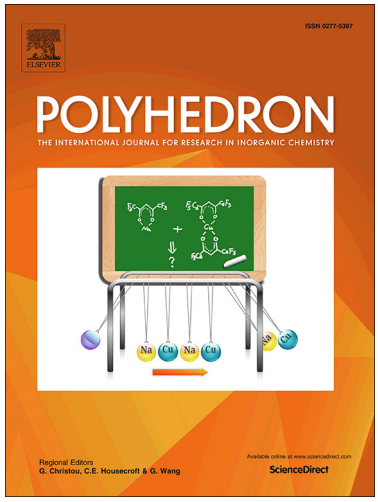

A neutral arene ruthenium(II) complex with a sulfonated N,O- chelating ligand: Synthesis, characterization, *in vitro* cytotoxicity and antibacterial activity

Gizem Selvi, Fethi Ahmet Ozdemir, Gurkan Aykutoglu, Namık Özdemir, Zafer Şerbetçi, Bekir Çetinkaya, Osman Dayan

PII: S0277-5387(19)30745-4
DOI: https://doi.org/10.1016/j.poly.2019.114300
Reference: POLY 114300

To appear in: *Polyhedron*

Received Date: 6 September 2019
Revised Date: 14 November 2019
Accepted Date: 17 November 2019

Please cite this article as: G. Selvi, F. Ahmet Ozdemir, G. Aykutoglu, N. Özdemir, Z. Şerbetçi, B. Çetinkaya, O. Dayan, A neutral arene ruthenium(II) complex with a sulfonated N,O- chelating ligand: Synthesis, characterization, *in vitro* cytotoxicity and antibacterial activity, *Polyhedron* (2019), doi: https://doi.org/10.1016/j.poly.2019.114300

A neutral arene ruthenium(II) complex with a sulfonated N,O-chelating ligand: Synthesis, characterization, *in vitro* cytotoxicity and antibacterial activity

Gizem Selvi[1], Fethi Ahmet Ozdemir[2], Gurkan Aykutoglu[2], Namık Özdemir[3], Zafer Şerbetçi[4], Bekir Çetinkaya[5], Osman Dayan[1*]

[1]Department of Chemistry, Faculty of Arts and Science, Çanakkale Onsekiz Mart University, Çanakkale, Turkey
[2]Department of Molecular Biology and Genetics, Faculty of Science and Art, Bingol University, Bingol, Turkey.
[3]Department of Mathematics and Science Education, Faculty of Education, Ondokuz Mayıs University, Samsun, Turkey
[4]Department of Chemistry, Faculty of Arts and Sciences, Bingol University, Bingol, Turkey
[5] Department of Chemistry, Ege University, Izmir, Turkey

Abstract

In this work, a new N,O- type ligand (**L1H**) containing a sulfonate ester group and its heteroleptic Ru(II) complex (**C1**) have been prepared and structurally characterized by various techniques, such as UV-vis, ESI-MS, NMR and IR. The spectroscopic results (IR, UV-vis and NMR) were compared with the results of density functional theory (DFT) calculations. The solid-state structures of **L1H** and **C1** were crystallographically verified. Moreover, the in vitro cytotoxicity and antibacterial properties of **1**, **L1H** and **C1** have been screened. All the compounds exhibited good cytotoxicity towards human neuroblastoma cancer cells and antibacterial effects towards 16 bacterial strains, both gram positive and negative. The results revealed that the Ru(II) complex exhibits higher biological activities than the starting materials **1** and **L1H**.

Keywords: Heteroleptic Ru(II) complex; sulfonated N,O- ligand; cytotoxicity; antibacterial activity.

*Corresponding author: Osman DAYAN

Email: osmandayan@comu.edu.tr

1. Introduction

There is increasing interest in arene ruthenium complexes because they have superior properties for many applications, such as catalysis, and in optical- and bio-materials [1-9]. These complexes generally prefer a piano-stool geometry (Figure 1). In this structure, various arenes can be used and the reactivity of the complex can be varied by using different mono- or bi-dentate ligands [5, 10, 11]. A frontier study with these compounds revealed that the $[Ru(C_6H_6)(DMSO)Cl_2]$ complex strongly inhibited topoisomerase II and showed anti-tumour activity [12]. Better cytotoxic activities have been achieved for (η^6-arene)Ru(II) complexes with a bidentate ligand compared to monodentate ligands [3, 13]. The amphiphilic character of the arene ruthenium unit and the hydrolysis propensity of the Ru-Z bonds to give '$Ru\text{-}OH_2$' species is essential for the cytotoxicity [7].

Although Sadler and co-workers have showed that (η^6-arene)Ru(II) complexes with chelating amino acid (N,O) ligands are inactive toward A2780 human ovarian cancer cell lines [14], researchers have demonstrated that (η^6-arene) Ru(II) complexes with other chelating N,O ligands exhibit cytotoxicity to different cancer cells [15]. Additionally, it has also been demonstrated that heteroleptic piano-stool Ru(II) complexes exhibit more selective biological activity and lower systematic toxicity than the square planar Pt(II) analogues [16].

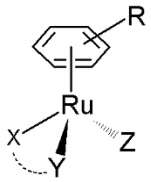

Figure 1. Arene Ru(II) complexes with a piano-stool geometry

On a different note, sulfonate esters are commonly used as a protecting group in organic syntheses [17-20]. Additionally, sulfonate esters have been investigated from the perspective of their biological properties [21-23]. The use of sulfonate esters in coordination chemistry is very rare. Recently, we have showed that Pd(II) and Ru(II) complexes containing aryl-sulfonate ester groups were good catalysts for the oxidation benzyl alcohol in the presence of H_5IO_6 [24]. Similarly, Chen and co-workers use Al catalysts including a sulfonate ester group in the ring opening polymerization of ε-caprolactone [25].

In the light of above information, we prepared a Ru(II) complex including a sulfonated Schiff base ligand and investigated its cytotoxic and antibacterial properties. The results indicated that this type of compound shows promising biological activities.

2. Experimental

2.1. General remarks

Information about the techniques, cytotoxic and antibacterial assays, crystal structure determination, along with the crystallographic data (Table S1), computational details and IR, NMR and MS spectra of the compounds are given in supporting information.

*2.2. Synthesis of **1***

Compound **1** was synthesized using the published procedure [26]. A mixture of salicylaldehyde (18.4 mmol, 2 mL) and triethylamine (36.8 mmol, 5 mL) in dichloromethane (20 ml) was stirred

under ambient conditions for 1 h. Then benzene-sulfonyl chloride (18.4 mmol) was added dropwise into the above solution and the resulting mixture was stirred under reflux overnight. The solvents were distilled until dryness. The precipitate thus obtained was washed with pure water and recrystallized from ethanol.

Yield: 77%; mp (°C): 60-62

FT-IR (ATR/cm^{-1}): 3074, 2896, 1694, 1601, 1578, 1477, 1449, 1401, 1374,1357, 1339, 1312, 1271, 1203, 1161, 1086, 1032, 997, 966, 934, 887, 868, 811, 785, 729, 699, 686.

^{1}H–NMR (300 MHz, $CDCl_3$) δ ppm: 7.21 (d, *J*=8.29 Hz, 1 H), 7.42 (t, *J*=7.72 Hz, 1 H), 7.51-7.67 (m, 3 H), 7.74 (t, *J*=7.54 Hz, 1 H), 7.86 (t, *J*=8.29 Hz, 2 H), 10.02 (s, 1 H).

^{13}C-NMR (75 MHz, $CDCl_3$) δ ppm: 123.6, 127.6, 128.4, 128.7, 129.2, 129.5, 134.3, 134.9, 135.3, 151.0, 187.1.

*2.3 Synthesis of the Schiff base ligand (**L1H**)*

An ethanolic solution of **1** (1 mmol) was combined with 2-hydroxyaniline (1 mmol) and refluxed for 24 h. The product was obtained on slow evaporation of the reaction mixture. It was purified by re-dissolving in ethanol and filtering, and then it was recrystallized.

Yield: 88%, mp (°C): 92-94

FT-IR (ATR/cm^{-1}): 3410, 3106, 3074, 3058, 3020, 2927, 1620, 1606, 1597, 1583, 1571, 1488, 1448, 1373, 1338, 1280, 1256, 1212, 1195, 1175, 1149, 1081, 1033, 963, 929, 869, 835, 776, 734, 695, 684.

^{1}H–NMR (300 MHz, $CDCl_3$) δ ppm: 6.88 (td, *J*=7.72, 1.51 Hz, 1 H), 6.95-7.01 (m, 1 H), 7.02-7.09 (m, 2 H), 7.16-7.24 (m, 2 H), 7.34-7.43 (m, 3 H), 7.43-7.50 (m, 1 H), 7.50-7.58 (m, 1 H), 7.73-7.82 (m, 2 H), 8.08 (dd, *J*=7.91, 1.88 Hz, 1 H), 8.53 (s, 1 H)

^{13}C-NMR (75 MHz, $CDCl_3$) δ ppm: 115.1, 116.0, 120.1, 123.8, 127.7, 128.1, 128.4, 129.3, 129.4, 129.6, 132.5, 134.7, 134.8, 135.2, 149.5, 150.7, 152.4.

*2.4 Synthesis of the Ru(II) complex (**C1**)*

The Schiff base ligand (**L1H**) (0.2 mmol) and triethyl amine (TEA) (0.2 mmol) were mixed in CH_2Cl_2 (10 mL) for 1h, then $[RuCl_2(p\text{-cymene})]_2$ (0.1 mmol) was added and the mixture was refluxed for 24 h. The volatiles were distilled until dryness at 50 °C. The crude product was washed with pure water (3x10 ml) and crystallized from a DCM/hexane mixture (1/3 v/v).

Yield: 39%, mp (°C): 224-226 (dec.)

FT-IR (ATR/cm^{-1}): 3061, 3034, 2966, 2924, 2869, 1594, 1579, 1557, 1472, 1448, 1374, 1325, 1289, 1262, 1230, 1198, 1166, 1140, 1085, 1029, 998, 951, 921, 881, 852, 792, 776, 743, 690.

^{1}H–NMR (400 MHz, $CDCl_3$) δ ppm: 1.20-1.26 (m, 6 H), 1.60 (s, 3 H), 2.94 (ddd, *J*=13.52, 7.03, 6.85 Hz, 1 H), 5.24 (d, *J*=5.62 Hz, 1 H), 5.46 (d, *J*=5.62 Hz, 1 H), 5.55 (d, *J*=6.32 Hz, 1 H), 5.58 (d, *J*=6.32 Hz, 1 H), 6.04-6.11 (m, 1 H), 6.65 (d, *J*=8.43 Hz, 1 H), 6.75 (d, *J*=8.43 Hz, 1 H), 6.91 (d, *J*=4.22 Hz, 1 H), 7.15 (t, *J*=7.03 Hz, 1 H), 7.19-7.25 (m, 1 H), 7.48 (dd, *J*=7.73, 2.11 Hz, 1 H), 7.51-7.54 (m, 1 H), 7.64-7.68 (m, 2 H), 7.79 (t, *J*=7.38 Hz, 1 H), 8.00 (dd, *J*=8.43, 1.40 Hz, 2 H), 8.92 (s, 1 H).

^{13}C-NMR (101 MHz, $CDCl_3$) δ ppm: 17.7, 20.9, 21.3, 29.6, 78.8, 79.1, 81.9, 85.7, 99.3, 100.0, 113.5, 114.5, 119.3, 121.0, 126.3, 127.3, 128.7, 129.6, 130.8, 130.9, 133.4, 134.0, 134.7, 137.1, 147.4, 153.4, 168.2.

Positive ESI–MS (*m*/*z*): 588.1 $[M–Cl]^+$.

Anal. Calc. for C1.H_2O: C, 54.3; H, 4.7; N, 2.2; found: C, 54.5; H, 4.9; N, 2.2%.

3. Results and discussion

In this work, a new N,O type ligand (**L1H**) was synthesized. For this, first salicylaldehyde was reacted with benzene-sulfonyl chloride in the presence of TEA, thus compound **1** was synthesized. Next, the new Schiff base was easily obtained from the reaction between compound **1** and 2-aminophenol in ethanol. If the salicylaldehyde is not sulfonated in first step, the resulting Schiff base might behave as a tridentate ligand [27]. In the last step, the Ru(II) complex (**C1**) was synthesized using the **L1H** ligand, TEA and [Ru(*p*-cymene)Cl_2]$_2$ (Scheme 1). The compounds were characterized using appropriate techniques, including NMR, IR, ESI-MS, CV and SC-XRD. The cell cytotoxicity and antibacterial activity of all the synthesized compounds were examined.

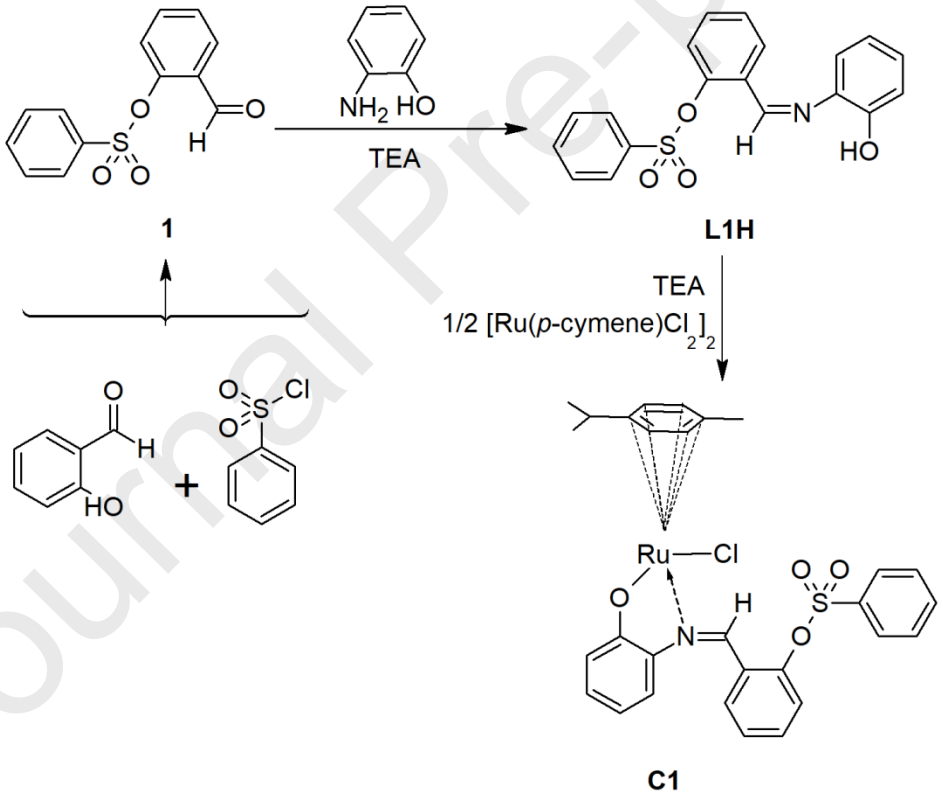

Scheme 1. Synthesis of the compounds

3.1. NMR spectroscopy

In the ^{1}H-NMR spectrum of compound **1**, the position of the –C*H*O proton was observed at δ 10.02 ppm. In the literature, this peak was reported at δ 10.14 ppm for the salicylaldehyde [28]. Other aromatic protons appeared in the δ 7.20-7.86 ppm region for **1**. For **L1H**, the –CH=N- peak appeared at δ 8.53 ppm and was calculated at δ 9.52 ppm. Other aromatic protons were around δ 6.88-8.08 ppm region for **L1H**, which were theoretically calculated to be in the range δ 7.15-8.69 ppm. The –OH proton was not observed in the ^{1}H-NMR spectrum of **L1H**, though it was seen at δ 7.27 ppm in the theoretical spectrum, i.e. within the region for the aromatic protons.

After the complexation of **L1H** with [Ru(*p*-cymene)Cl_2]$_2$ in the presence of TEA, the –CH=N- proton markedly shifted downfield to δ 8.92 ppm and was calculated at δ 9.53 ppm for **C1**. In the complex, the aromatic protons belonging to the **L1** fragment appeared around δ 6.02-8.00 ppm, which were theoretically found in the range δ 6.55-9.52 ppm. Aromatic –C*H* protons belonging to the *p*-cymene group appeared around δ 5.24-5.58 ppm and the -C*H*(CH_3)$_2$ protons were observed at δ 2.94 ppm. These chemical shifts were calculated as the δ 3.78-6.10 ppm range and δ 2.85 ppm, respectively. The -C*H*$_3$ protons were observed in the δ 1.22-1.60 ppm region, while these were calculated to fall in the range δ 0.93-3.30 ppm.

In the ^{13}C-NMR spectrum of compound **1**, the position of –*C*HO carbon atom was at δ 187.1 ppm. For **L1H**, the -CH=N- carbon atom was observed at δ 152.4 ppm and it was calculated to be at δ 157.79 ppm. Similarly, the -CH=N- carbon atom was observed at δ 153.4 ppm for **C1**. Additionally, carbon peaks were compatible with the expectations for **1**, **L1H** and **C1**. All the NMR spectra are given in the supplementary file.

3.2. IR spectroscopy

In the FT-IR spectrum of **1**, the C=O stretching frequency was observed at 1694 cm^{-1}. The C-H stretching frequency belonging to the aldehyde group of compound **1** was 2896 cm^{-1}. While the

symmetrical O=S=O vibration appeared at 1161 cm^{-1} for **1**, the asymmetrical one appeared at 1374 cm^{-1}. On the other hand, the S-O stretching vibration was observed at 868 cm^{-1}. The aromatic C-H vibrations were observed at 3074 cm^{-1}.

For **L1H**, the O-H stretching vibration was observed at 3410 cm^{-1} and calculated to be 3537 cm^{-1}. The -C=N- stretching vibration was observed at 1620 cm^{-1} for **L1H**, which coincides with the theoretical value of 1619 cm^{-1}. The symmetrical (1175 cm^{-1}) and asymmetrical (1373 cm^{-1}) O=S=O and S-O stretching (869 cm^{-1}) vibrations are slightly shifted compared to compound **1**. These bands appeared at 1108, 1283 and 641 cm^{-1} in the theoretical spectrum, respectively. The vibrations in the 3106-3020 cm^{-1} region are attributed to the aromatic C-H stretching vibrations, which were calculated as being 3107 and 3013 cm^{-1}. The C-H stretching vibrations belonging to the aldimine group of compound **1** were observed at 2896 cm^{-1}.

For **C1**, the –C=N- stretching vibration shifted toward 1594 cm^{-1} experimentally and toward 1587 cm^{-1} computationally. The symmetrical (1166 cm^{-1}) and asymmetrical (1374 cm^{-1}) O=S=O and S-O stretching (852 cm^{-1}) vibrations are very close to those of **L1H**. These vibrations were predicted at 1107, 1277 and 649 cm^{-1} in the theoretical spectrum, respectively. The aromatic and aliphatic C-H stretching vibrations were observed in the 3061-3034 and 2966-2924 cm^{-1} regions, and these were calculated to be in the 3111-3043 and 3033-2923 cm^{-1} regions, respectively. The theoretical and experimental FT-IR spectra of the compounds are given in the supplementary file.

3.3. UV-vis spectroscopy

In the UV-vis spectrum of compound **1** (

Figure 2a), there are two bands under 300 nm, corresponding to intra-ligand $\pi \rightarrow \pi^*$ transitions. In the Schiff base (**L1H**), a new intra-ligand $\pi \rightarrow \pi^*$ transition was observed in the 300-400 nm region. According to TD-DFT calculations of **L1H**, an absorption was predicted at 379 nm with a

major contribution from the HOMO to LUMO transition (97%), in which the energy difference between the HOMO and LUMO is 3.67 eV. Additionally, the Ru(II) complex (**C1**) had a new metal to ligand charge transfer (MLCT ($4d \rightarrow \pi^*$)) band in the 480-580 nm region. The optical band gap (E_{bg}) of **C1** obtained from absorption spectrum was similar to that calculated by the reported method, being 1.82 eV [29]. The TD-DFT calculation shows that the theoretical UV-vis spectrum of **C1** includes an absorption peak at 462 nm, with the major contributions originating from HOMO to LUMO (42%), HOMO to LUMO+2 (25%) and from HOMO to LUMO+3 (14%), in which the energy difference between the HOMO and LUMO is 3.03 eV. The optimal molecular structure and iso-density surface plots of the frontier molecular orbitals for **L1H** and **C1**, calculated by DFT, are given in the supporting information.

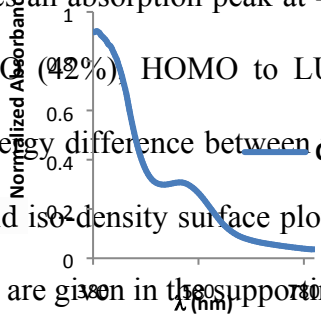

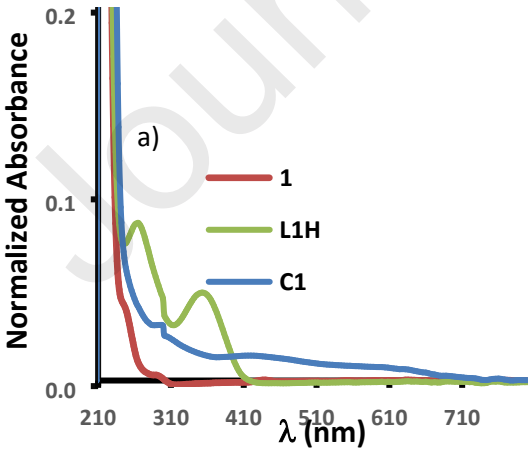

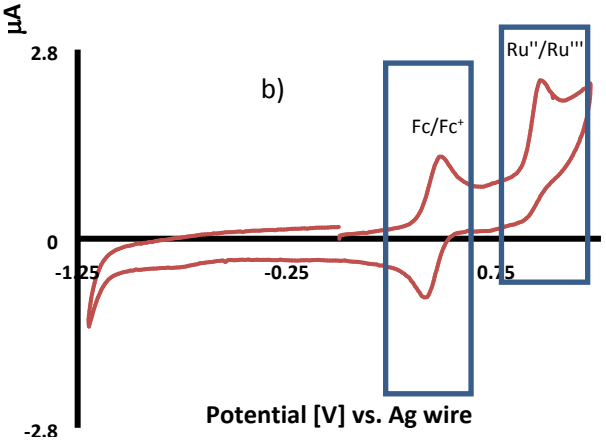

Figure 2. (a) The normalized UV-vis spectra of compounds **1**, **L1H** and **C1** in MeOH. (b) Cyclic voltammogram of the **C1** complex measured in DMF solution (1 x 10^{-3}M) at a scan rate of 100 mVs^{-1}.

3.4. Electrochemical properties

The electrochemical properties of the Ru(II) complex (**C1**) were investigated by the cyclic voltammetry technique using a three electrode system. The voltammogram is depicted in

Figure 2b. According to the voltammogram, **C1** exhibits an irreversible oxidation peak at + 0.86 V vs Ag wire. The peak at +0.86 V was attributed to the Ru(II) / Ru(III) couple [30]. Additionally, the oxidation peak of the Fc/Fc^+ redox couple appeared at + 0.36 V in this system. As a result, the energy level of HOMO was estimated to be -5.30 eV using the equation E_{HOMO} (eV) = -(E_{ox}^{onset} - E_{Fc/Fc^+}^{onset}) - 4.8 eV [31] and the energy level of the LUMO was calculated as -3.48 eV using the equation $E_{LUMO} = E_{HOMO} + E_{bg}$ [32, 33].

3.5. Crystal structures

The solid-state structures of the Schiff base ligand (**L1H**) and the Ru(II) complex (**C1**) were determined with the SC-XRD technique. The crystal data and structure refinement parameters are given in Table 1.

Table 1. Crystal data and structure refinement parameters for **L1H** and **C1**.

Parameters	**L1H**	**C1**
CCDC depository	1895130	1895131
Color/shape	Prism/light yellow	Prism/dark red
Chemical formula	$C_{19}H_{15}NO_4S$	$[RuCl(C_{10}H_{14})(C_{19}H_{14}NO_4S]\cdot CH_2Cl_2$
Formula weight	353.38	708.03
Temperature (K)	296(2)	293(2)
Wavelength (Å)	0.71073 Mo Kα	0.71073 Mo Kα
Crystal system	Monoclinic	Triclinic
Space group	$P2_1/c$ (No. 14)	$P\bar{1}$ (No. 2)
Unit cell parameters		
a, *b*, *c* (Å)	18.5563(7), 14.8008(9), 18.6047(7)	10.6329(7), 12.0507(9), 12.9282(10)

α, β, γ (°)	90, 102.729(3), 90	96.299(6), 90.305(6), 112.470(5)
Volume (Å^3)	4984.2(4)	1519.5(2)
Z	12	2
$D_{calc.}$ (g/cm^3)	1.413	1.547
μ (mm^{-1})	0.219	0.884
Absorption correction	Integration	
$T_{min.}$, $T_{max.}$	0.8979, 0.9344	0.6113, 0.8264
F_{000}	2208	720
Crystal size (mm^3)	0.54 × 0.54 × 0.38	0.44 × 0.21 × 0.08
Diffractometer/measurement	STOE IPDS II/ω scan	
Index ranges	$-22 \le h \le 22$, $-17 \le k \le 17$, $-22 \le l \le 22$	$-13 \le h \le 13$, $-15 \le k \le 15$, $-16 \le l \le 16$
θ range for data collection (°)	$1.775 \le \theta \le 25.050$	$1.842 \le \theta \le 27.577$
Reflections collected	63689	16882
Independent/observed reflections	8841/3062	6983/5638
$R_{int.}$	0.1135	0.0474
Refinement method	Full-matrix least-squares on F^2	
Data/restraints/parameters	8841/0/676	6983/0/364
Goodness-of-fit on F^2	0.884	1.016
Final R indices [$I > 2\sigma(I)$]	$R_1 = 0.0963$, $wR_2 = 0.2118$	$R_1 = 0.0354$, $wR_2 = 0.0886$
R indices (all data)	$R_1 = 0.2013$, $wR_2 = 0.2678$	$R_1 = 0.0487$, $wR_2 = 0.0956$
$\Delta\rho_{max.}$, $\Delta\rho_{min.}$ (e/Å^3)	1.41, −0.31	0.69, −0.41

L1H crystallizes with twelve molecules per asymmetric unit, in the monoclinic crystal system with the space group $P2_1/c$. Its solid-state structure is shown in Figure 3, while important bond lengths and angles are reported in Table S1. There are three molecules in the asymmetric unit of **L1H**, labelled as A, B and C. For clarity, only A is plotted in Figure 3.

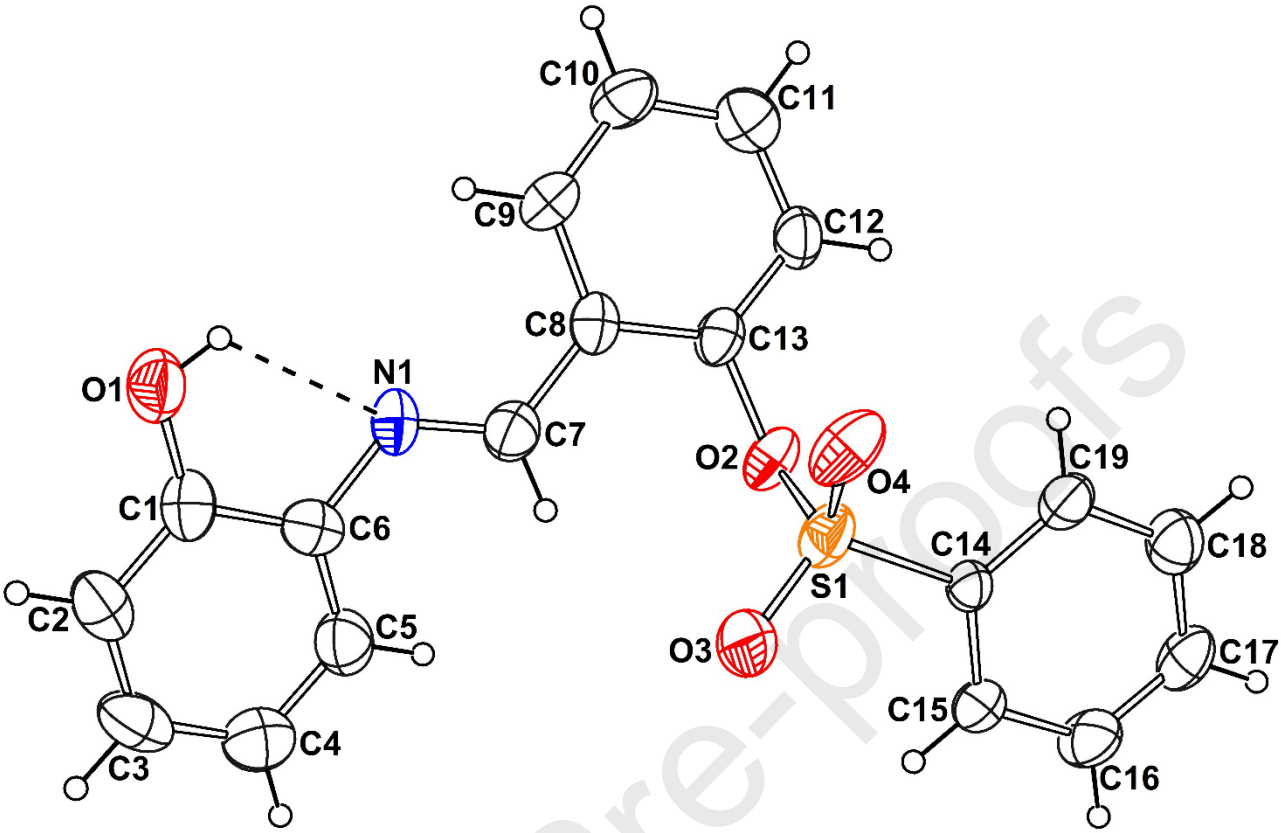

Figure 3. A molecule of **L1H** showing the atom-numbering scheme. Displacement ellipsoids are drawn at the 30% probability level and H atoms are shown as small spheres of arbitrary radii. An intramolecular H-bond is represented by a dashed line.

In **L1H**, the average O1─C1 and N1─C6 distances of 1.346 and 1.409 Å, respectively, correspond to single bond lengths while the average N1─C7 distance of 1.265 Å is consistent with N═C double bonding. These bonds are calculated as 1.352, 1.403 and 1.281 Å, respectively. All the interatomic distances and angles show no unusual values [34] and are comparable with those in similar structures [35-39].

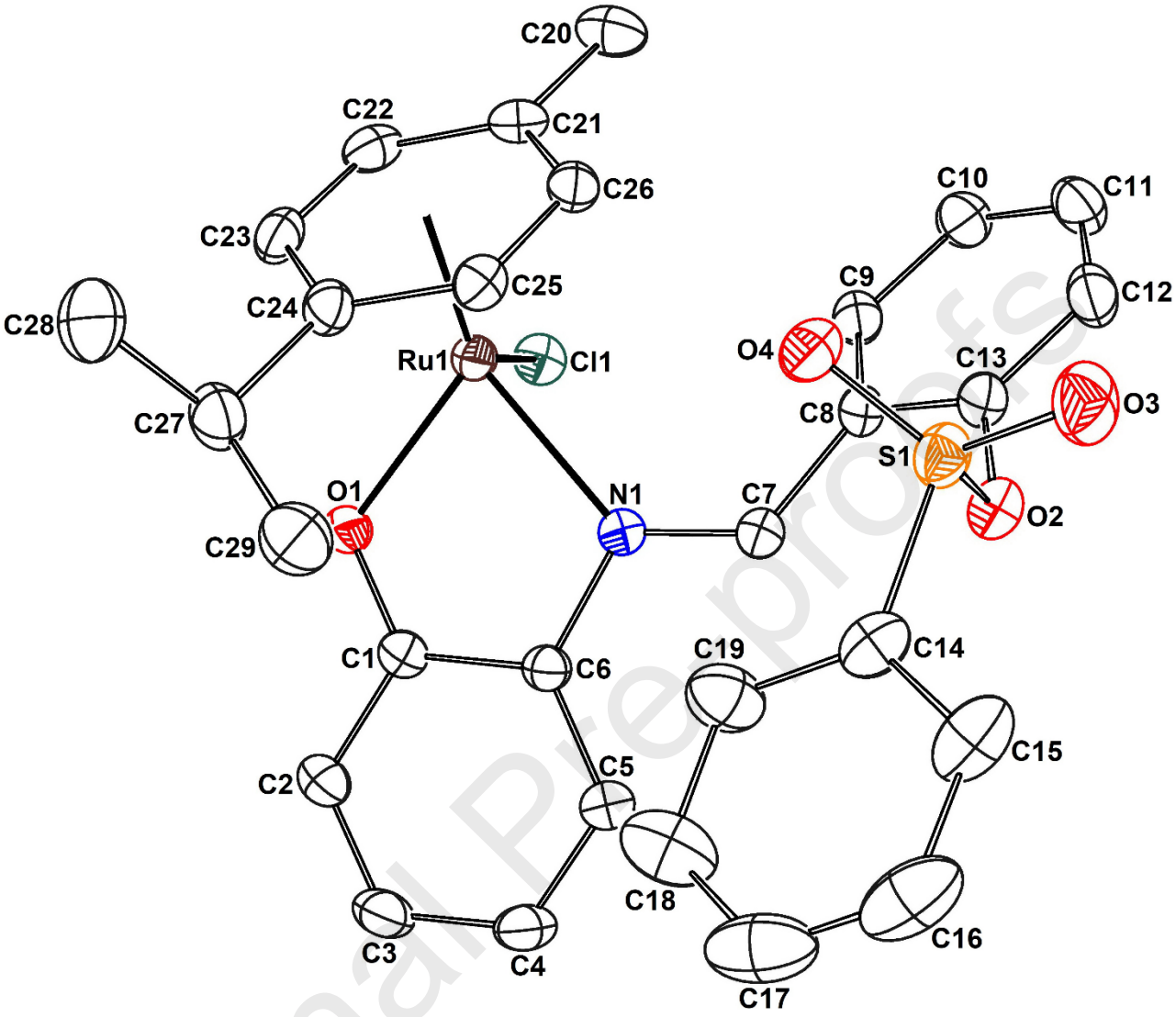

Figure 4. Perspective view of the asymmetric unit of **C1** showing the atom-numbering scheme. Displacement ellipsoids are drawn at the 20% probability level. The dichloromethane solvent molecule and H atoms are omitted for clarity.

The ORTEP-3 diagram of **C1** is shown in Figure 4, while selected bond lengths and bond angles are given in Table S1. The complex crystallized with a dichloromethane solvent molecule in the triclinic space group $P\bar{1}$, with two molecules per unit cell. **C1** has a piano-stool geometry, like many half-sandwich Ru(II) arene complexes [40-44]. In this case, while the nitrogen and

oxygen atoms of **L1**$^{-}$ and the chloride ligand form the three legs of the piano stool, the *p*-cymene ring forms the seat of the piano-stool. The Ru(II) ion is π-bonded to the *p*-cymene ring in a η^6-coordination mode, and in this geometry, the atoms Cl1, O1 and N1 eclipse the arene C─C bonds rather than the C atoms when viewed along the arene centroid─Ru bond axis.

The Ru center has a quasi-octahedral coordination geometry, assuming that the *p*-cymene ring serves as a three-coordinated ligand. Alternatively, the coordination geometry around the metal atom may be regarded as a tetrahedron, treating the center of the *p*-cymene aromatic ring as the fourth ligand position. If *Cg* is the centroid of the aromatic ring, the Ru─*Cg* distance is found to be 1.6685(2) Å, and the Cl1─Ru1─*Cg*, O1─Ru1─*Cg* and N1─Ru1─*Cg* angles are 127.76(2), 126.13(6) and 132.69(6)°, respectively. The Cl1─Ru1─O1, Cl1─Ru1─N1 and O1─Ru1─N1 angles (mean 84.55°) are smaller than the ideal tetrahedral angle (109.47°), which is counterbalanced by the expansion of the *Cg*─Ru─*L* (L is Cl1, O1 or N1) angles (mean 128.86°).

The O- and N-donor atoms of the **L1H** ligand form a five-membered metallacycle (containing the atoms O1/C1/C6/N1/Ru1) with the r.m.s deviation from the plane being 0.0622 Å. The experimental Ru─Cl1, Ru1─O1 and Ru1─N1 bond distances are found to be 2.4149(7), 2.0576(17) and 2.129(2) Å, and they are calculated as 2.482, 2.056 and 2.161 Å, respectively. Also, the Ru─C lengths change from 2.162(3) to 2.228(3) Å, while these bonds theoretically vary from 2.190 to 2.296 Å. Many Ru(II)-arene complexes with same coordination environment have been reported crystallographically [40-44]. According to the bond lengths in these structures, the Ru─*Cg*, Ru─C, Ru─Cl, Ru─O and Ru─N bond lengths vary from 1.657 to 1.677, 2.157 to 2.223, 2.416 to 2.441, 2.044 to 2.067 and 2.075 to 2.104 Å, respectively. These values mean that the coordination bonds of **C1** match well with the literature values.

When the bond lengths in **L1H** and **C1** are compared, it is seen that the coordination elongates the mean N1─C6 and mean N1─C7 bond distances from 1.409 to 1.439 Å and from

1.265 to 1.291 Å, respectively, while the coordination contracts the mean O1─C1 bond from 1.346 to 1.301 Å. In addition, coordination of N1 causes an increase in the N1─C7─C8 bond angle (from mean 122.93 to 127.6°) and a decrease in the C6─N1─C7 bond angle (from mean 122.67 to 118.4°), while the bond angles around the coordinating O1 atom remain almost unchanged. Similar trends are also seen in the theoretical values.

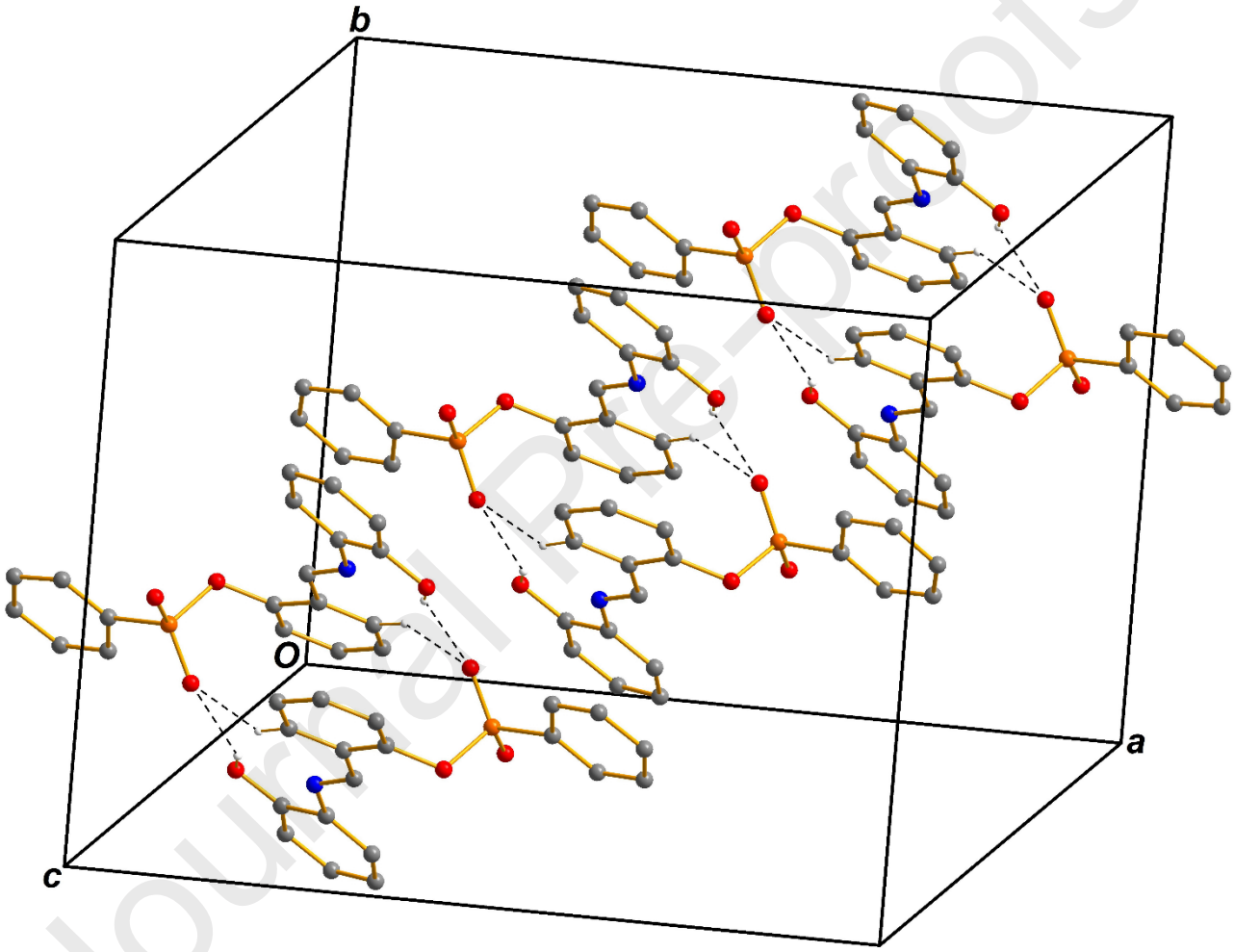

Figure 5. Part of the crystal structure of **L1H** showing the intermolecular interactions. For the sake of clarity, only H atoms involved in hydrogen bonding have been included.

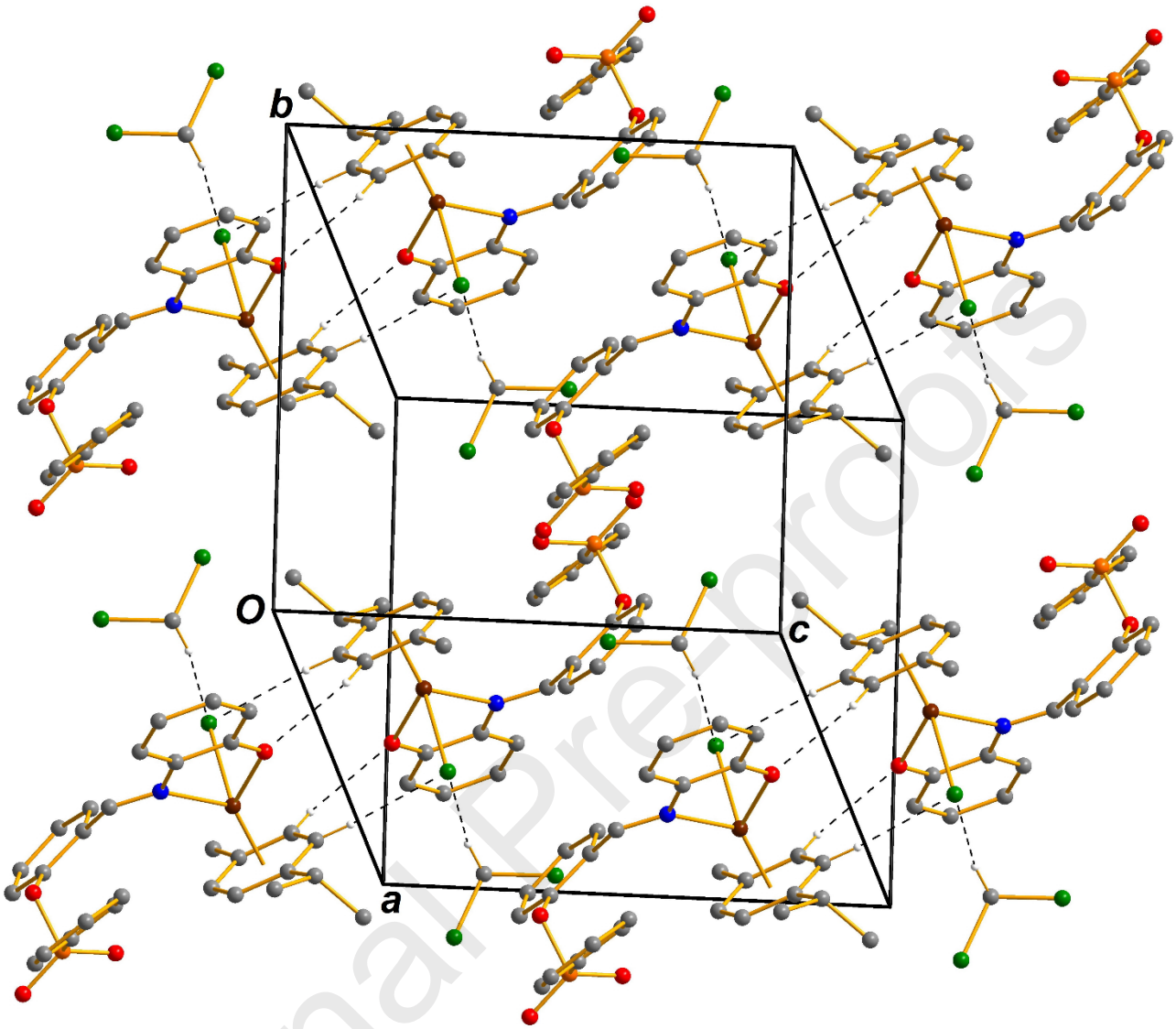

Figure 6. Part of the crystal structure of **C1** showing the intermolecular interactions. For the sake of clarity, only H atoms involved in hydrogen bonding have been included.

In the molecular structure of **L1H**, an intramolecular O1─H1···N1 contact leads to the formation of a five-membered ring (Figure 3). In the crystal structure, the atoms C9 and O1 act as hydrogen-bond donors, *via* atoms H9 and H1, to atom O4 in the inversion-related molecule (

Figure 5), thus forming a centrosymmetric dimeric unit. In the molecular structure of **C1**, intramolecular C9─H9···Cl1 and C25─H25···O4 contacts lead to the formation of seven- and ten-membered rings, respectively. In the crystal structure, the dichloromethane solvent molecule is connected to the complex molecule by a C30─H30A···Cl1 hydrogen bond. Furthermore, atoms C22 and C23 act as hydrogen-bond donors, *via* atoms H22 and H23, to atoms O1 and Cl1, respectively, in the inversion-related complex molecule (Figure 6), thus generating a centrosymmetric dimeric unit. Details of the non-covalent interactions are given in Table S2.

3.6. Cell cytotoxicity analysis

The cytotoxic activities of Ru(II) complexes containing bidentate NO^- chelating ligands are well-known in the literature [41, 45-55]. The cytotoxic activity of these complexes mainly depends on two factors: The first is the contribution of other ligands in the complex. Ru(II) complexes containing NO^- chelating ligands show good cytotoxic activity in the presence of a slow-leaving ligand, such as *p*-cymene, and a fast-leaving ligand, such as Cl^- [48, 56-58]. The second factor is the effects of the NO^- chelating ligands. The number of members in the chelate ring, as well as the steric and electronic parameters of the ligands, are important [41, 49, 50, 59, 60]. While the cytotoxic activities of (NO^-)Ru(II) complexes including 6-membered chelate rings have been widely studied in the literature, studies on complexes with 5-membered chelate rings are rare. In light of this information, the cytotoxic properties of the synthesized **C1** complex, which includes a 5-membered chelate ring, and the ligands **1** and **L1H** were investigated.

For this purpose, SH-SY5Y cells were treated with the synthesized compounds, at various doses (7, 15, 31, 62.5, 125, 250, 500 µg/ml), for 24 h (Figure 7). All thcompounds exhibited cytotoxic effects on human SH-SY5Y cancer cells at different doses compared with the control group. Compound **1** exhibited cytotoxic activity at 31-500 ug/ml doses, but the optimum dose was 62.5

μg/ml. For **L1H**, the cytotoxic activity was seen at 31 and 62.5 μg/mL, and optimum dose was 62.5 μg/mL, like compound **1**. On the other hand, it was observed that the ruthenium complex (**C1**) showed cytotoxic activity at 15-62.5 μg/ml doses and the optimum dose was 31 μg/ml. When compounds **1**, **L1H** and **C1** were compared, the ruthenium complex (**C1**) showed cytotoxic activity at a lower dose.

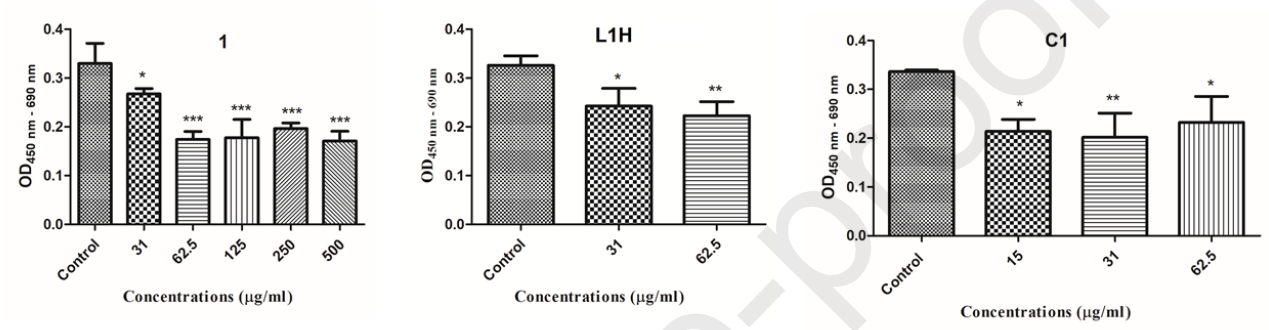

Figure 7. WST-1 results of chemicals on SH-SY5Y human neuroblastoma cells for 24 h. Cells were cultured and exposed to different doses of the synthesized compounds for 24 h. Control groups contain just growth media (Statistical analysis were carried out by One-way ANOVA and the Dunnet test using the Graphpad Prism 5 program. Data were expressed as mean+SD and * $p<0.05$, ** $p<0.01$, ***$p<0.001$ vs Control and n=4).

3.7. Antibacterial Activity Analysis

The antibacterial activities of the synthesized compounds were tested in vitro against 16 bacterial species (7 gram-positive and 9 gram-negative) (Table 2). The results are summarized below:

- All the synthesized compounds showed efficient antibacterial activity on gram positive bacteria.

- In general, the compounds were more efficient on gram positive bacteria than gram negative bacteria.
- Compound **1** did not show any antibacterial activity on gram negative bacteria.
- For **1**, **L1H** and **C1**, the antibacterial efficiency on all bacterial species follows the order: **C1** > **L1H** > **1**.
- The **C1** has better antibacterial efficiency on both gram-positive and gram-negative bacterial species than the other compounds.

Table 2. Antibacterial activity of the synthesized compounds using the disc diffusion method.

Bacteria	**Gram**	**İnhibition zone diameter (mm)**			
		1	**L1H**	**C1**	DMSO (Control)
Bacillus subtilis ATCC 6337	Positive	5	8	**11**	-
Brevibacillus brevis	Positive	7	10	**13**	
Bacillus megaterium DSM 32	Positive	6	9	**10**	
Bacillus subtilis IM 622	Positive	3	7	**9**	
Bacillus cereus EMC 19	Positive	6	6	**12**	
Staphylococcus aureus 6538 P	Positive	7	11	**13**	
Listeria monocytogenes NCTC 5348	Positive	5	8	**11**	
Salmonella typhimurium NRRLE 4413	Negative	-	4	**7**	
Pseudomonas fluorescens	Negative	-	6	**8**	
Enterobacter aerogenes CCM 2531	Negative	-	3	**5**	
Klebsiella pneumoniae EMCS	Negative	-	5	**8**	
Escherichia coli ATCC 25922	Negative	-	7	**9**	
Proteus vulgaris FMC II	Negative	-	4	**6**	
Pseudomonas aeruginosa DSM 50070	Negative	-	3	**7**	
Proteus vulgaris	Negative	-	4	**5**	
Salmonella enterica ATCC 13311	Negative	-	5	**8**	

4. Conclusion

In this work, a new N,O-type bidentate Schiff base ligand bearing an aryl sulfonate ester group and its heteroleptic Ru(II) arene complex were synthesized and characterized with NMR, IR, UV and CV as well as single crystal X-ray diffraction techniques. The single crystal X-ray diffraction technique shows that the N,O ligand (**L1H**) crystallizes in the monoclinic crystal system with the

$P2_1/c$ space group and has three molecules in the asymmetric unit. On the other hand, the Ru(II) complex prefers a piano-stool geometry in the solid state and crystallizes in the triclinic space group $P\bar{1}$. The cytotoxic and antibacterial properties of the synthesized compounds were investigated. All the compounds show cytotoxicity against the human neuroblastoma cancer cell (SH-SY5Y) and an antibacterial effect on 16 bacterial species, including gram-positive and gram-negative species. The results showed that the Ru(II) complex (**C1**) has a greater cytotoxic effect at a low dose. Additionally, all the compounds show antibacterial effects toward different bacterial species. However, the Ru(II) complex has a greater antibacterial effect than ligands **L1H** and **1** for the studied bacterial species.

Appendix A. Supplementary data

CCDC 1895130 and 1895131 contain the supplementary crystallographic data for the compounds reported in this article. These data can be obtained free of charge on application to CCDC, 12 Union Road, Cambridge CB2 1EZ, UK [Fax: +44 1223 336 033, e-mail: deposit@ccdc.cam.ac.uk, https://www.ccdc.cam.ac.uk/structures/].

Acknowledgements

This study was supported by Çanakkale Onsekiz Mart University (Project No: FYL-2019-2883) and Ondokuz Mayıs University (Project No: PYO.FEN.1906.19.001). We also thank Amasya University, Turkey, for the use of GaussView 5.0 and the Gaussian 09 program package. Bekir Çetinkaya thanks the Turkish Academy of Science (TUBA) for support.

References

[1] R. Noyori, S. Hashiguchi, Asymmetric Transfer Hydrogenation Catalyzed by Chiral Ruthenium Complexes, Acc. Chem. Res., 30 (1997) 97-102.
[2] A.J. Davenport, D.L. Davies, J. Fawcett, S.A. Garratt, D.R. Russell, Arene ruthenium complexes with pyridyloxazolines: synthesis and applications as asymmetric catalysts for Diels-Alder reactions, J Chem Soc, Dalton Trans., (2000) 4432-4441.
[3] R.E. Morris, R.E. Aird, P. del Socorro Murdoch, H. Chen, J. Cummings, N.D. Hughes, S. Parsons, A. Parkin, G. Boyd, D.I. Jodrell, P.J. Sadler, Inhibition of Cancer Cell Growth by Ruthenium(II) Arene Complexes, J. Med. Chem., 44 (2001) 3616-3621.
[4] C. Berg, S. Chari, K. Jurgaityte, A. Laurora, M. Naldony, F. Pope, D. Romano, T. Medupe, S. Prince, S. Ngubane, J. Baumgartner, B. Blom, Modulation of the solubility properties of arene ruthenium complexes bearing stannyl ligands as potential anti-cancer agents, J. Organomet. Chem., 891 (2019) 12-19.
[5] C. Scolaro, A. Bergamo, L. Brescacin, R. Delfino, M. Cocchietto, G. Laurenczy, T.J. Geldbach, G. Sava, P.J. Dyson, In Vitro and in Vivo Evaluation of Ruthenium(II)−Arene PTA Complexes, J. Med. Chem., 48 (2005) 4161-4171.
[6] Y.K. Yan, M. Melchart, A. Habtemariam, P.J. Sadler, Organometallic chemistry, biology and medicine: ruthenium arene anticancer complexes, Chem. Commun., (2005) 4764-4776.
[7] G. Süss-Fink, Arene ruthenium complexes as anticancer agents, Dalton Trans., 39 (2010) 1673-1688.
[8] P. Zhang, P.J. Sadler, Advances in the design of organometallic anticancer complexes, J. Organomet. Chem., 839 (2017) 5-14.
[9] F. Zobi, B.B. Mood, P.A. Wood, F.P.A. Fabbiani, S. Parsons, P.J. Sadler, Tagging (Arene)ruthenium(II) anticancer complexes with fluorescent labels, Eur. J. Inorg. Chem., (2007) 2783-2796.
[10] M.J. Clarke, Ruthenium metallopharmaceuticals, Coord. Chem. Rev., 236 (2003) 209-233.
[11] I. Berger, M. Hanif, A.A. Nazarov, C.G. Hartinger, R.O. John, M.L. Kuznetsov, M. Groessl, F. Schmitt, O. Zava, F. Biba, V.B. Arion, M. Galanski, M.A. Jakupec, L. Juillerat-Jeanneret, P.J. Dyson, B.K. Keppler, In Vitro Anticancer Activity and Biologically Relevant Metabolization of Organometallic Ruthenium Complexes with Carbohydrate-Based Ligands, Chem. Eur. J., 14 (2008) 9046-9057.
[12] Y.N.V. Gopal, D. Jayaraju, A.K. Kondapi, Inhibition of Topoisomerase II Catalytic Activity by Two Ruthenium Compounds: A Ligand-Dependent Mode of Action, Biochemistry, 38 (1999) 4382-4388.
[13] R.E. Aird, J. Cummings, A.A. Ritchie, M. Muir, R.E. Morris, H. Chen, P.J. Sadler, D.I. Jodrell, In vitro and in vivo activity and cross resistance profiles of novel ruthenium(II) organometallic arene complexes in human ovarian cancer, Br. J. Cancer, 86 (2002) 1652-1657.
[14] A. Habtemariam, M. Melchart, R. Fernández, S. Parsons, I.D.H. Oswald, A. Parkin, F.P.A. Fabbiani, J.E. Davidson, A. Dawson, R.E. Aird, D.I. Jodrell, P.J. Sadler, Structure−Activity Relationships for Cytotoxic Ruthenium(II) Arene Complexes Containing N,N-, N,O-, and O,O-Chelating Ligands, J. Med. Chem., 49 (2006) 6858-6868.
[15] L. Zeng, P. Gupta, Y. Chen, E. Wang, L. Ji, H. Chao, Z.-S. Chen, The development of anticancer ruthenium(ii) complexes: from single molecule compounds to nanomaterials, Chem. Soc. Rev., 46 (2017) 5771-5804.
[16] H. Chen, J.A. Parkinson, R.E. Morris, P.J. Sadler, Highly Selective Binding of Organometallic Ruthenium Ethylenediamine Complexes to Nucleic Acids: Novel Recognition Mechanisms, J. Am. Chem. Soc., 125 (2003) 173-186.
[17] M.S. Alam, S. Koo, Deprotection of durable benzenesulfonyl protection for phenols — efficient synthesis of polyphenols, Synth. Commun., 48 (2018) 247-254.
[18] M.S. Shashidhar, M.V. Bhatt, 2-Formylbenzenesulphonyl chloride as a reagent for the protection of phenols, J. Chem. Soc., Chem. Commun., (1987) 654-656.
[19] A. Briot, C. Baehr, R. Brouillard, A. Wagner, C. Mioskowski, Benzylsulfonyl: a valuable protecting and deactivating group in phenol chemistry, Tetrahedron Lett., 44 (2003) 965-967.

[20] H. Maeda, K. Yamamoto, I. Kohno, L. Hafsi, N. Itoh, S. Nakagawa, N. Kanagawa, K. Suzuki, T. Uno, Design of a Practical Fluorescent Probe for Superoxide Based on Protection–Deprotection Chemistry of Fluoresceins with Benzenesulfonyl Protecting Groups, Chem. Eur. J., 13 (2007) 1946-1954.
[21] X. Lin, D. Tian, Y. Fu, Y. Li, L. Huang, W. Gu, J. Song, Y. Li, Y. Ben-David, M. Wen, C. Yuan, X. Hao, Synthesis of novel guttiferone E and xanthochymol derivatives with cytotoxicities by inducing cell apoptosis and arresting the cell cycle phase, Eur. J. Med. Chem., 162 (2019) 765-780.
[22] S.L. Gwaltney, H.M. Imade, K.J. Barr, Q. Li, L. Gehrke, R.B. Credo, R.B. Warner, J.Y. Lee, P. Kovar, J. Wang, M.A. Nukkala, N.A. Zielinski, D. Frost, S.-C. Ng, H.L. Sham, Novel sulfonate analogues of combretastatin A-4: potent antimitotic agents, Bioorg. Med. Chem. Lett., 11 (2001) 871-874.
[23] Y.-N. Shen, L. Lin, H.-Y. Qiu, W.-Y. Zou, Y. Qian, H.-L. Zhu, The design, synthesis, in vitro biological evaluation and molecular modeling of novel benzenesulfonate derivatives bearing chalcone moieties as potent anti-microtubulin polymerization agents, RSC Adv., 5 (2015) 23767-23777.
[24] R. Kağıt, O. Dayan, N. Özdemir, Palladium(II) and Ruthenium(II) complexes bearing arylsulfonate based ligands: Synthesis, structural characterization and catalytic properties, Polyhedron, 117 (2016) 504-512.
[25] C.-L. Lee, Y.-F. Lin, M.-T. Jiang, W.-Y. Lu, J.K. Vandavasi, L.-F. Wang, Y.-C. Lai, M.Y. Chiang, H.-Y. Chen, Improvement in Aluminum Complexes Bearing Schiff Bases in Ring-Opening Polymerization of ε-Caprolactone: A Five-Membered-Ring System, Organometallics, 36 (2017) 1936-1945.
[26] E.M. Chen, P.-J. Lu, A.Y. Shaw, Synthesis and Antiproliferative Evaluation of 2'-Arenesulfonyloxy-5-benzylidene-thiazolidine-2,4-diones, J. Heterocycl. Chem., 49 (2012) 792-798.
[27] J. Xiang, L.-H. Jia, W.-L. Man, K. Qian, G.-H. Lee, S.-M. Peng, S.-M. Yiu, S. Gao, T.-C. Lau, A novel triazidoruthenium(iii) building block for the construction of polynuclear compounds, Dalton Trans., 41 (2012) 5794-5798.
[28] M.M. Raymond J. Abraham, 1H Chemical Shifts and Structural Chemistry: Theory, Applications and NMR Prediction Software, in, Wiley, Chichester, 2008.
[29] O. Dayan, N. Ozdemir, F. Yakuphanoglu, Z. Serbetci, A. Bilici, B. Cetinkaya, M. Tercan, Synthesis and photovoltaic properties of new Ru(II) complexes for dye-sensitized solar cells, J. Mater. Sci. Mater. El., 29 (2018) 11045-11058.
[30] E. Stein, S.Y. Oki, E.J.S. Vichi, Synthesis and electrochemical characterization of bimetallic ruthenium complexes with the bridging h2(s,s)-1,3-butadiyne-1,4-diyl ligand, J. Braz. Chem. Soc., 11 (2000) 252-256.
[31] C. Fujisue, T. Kadoya, T. Higashino, R. Sato, T. Kawamoto, T. Mori, Air-stable ambipolar organic transistors based on charge-transfer complexes containing dibenzopyrrolopyrrole, RSC Adv., 6 (2016) 53345-53350.
[32] B. Chen, Y.H. Li, W. Yang, W. Luo, H.B. Wu, Efficient sky-blue and blue-green light-emitting electrochemical cells based on cationic iridium complexes using 1,2,4-triazole-pyridine as the ancillary ligand with cyanogen group in alkyl chain, Org. Electron., 12 (2011) 766-773.
[33] Z.Z. Lu, J.D. Peng, A.K. Wu, C.H. Lin, C.G. Wu, K.C. Ho, Y.C. Lin, K.L. Lu, Heteroleptic Ruthenium Sensitizers with Hydrophobic Fused-Thiophenes for Use in Efficient Dye-Sensitized Solar Cells, Eur. J. Inorg. Chem., (2016) 1214-1224.
[34] F.H. Allen, O. Kennard, D.G. Watson, L. Brammer, A.G. Orpen, R. Taylor, Tables of Bond Lengths Determined by X-Ray and Neutron-Diffraction .1. Bond Lengths in Organic-Compounds, J. Chem. Soc., Perkin Trans. 2, (1987) S1-S19.
[35] N. Ozdemir, R. Kagit, O. Dayan, Investigation of enol-imine/keto-amine tautomerism in (E)-4-[(2-hydroxybenzylidene)amino]phenyl benzenesulphonate by experimental and molecular modelling methods, Mol. Phys., 114 (2016) 757-768.
[36] D. Kand, P.S. Mandal, T. Saha, P. Talukdar, Structural imposition on the off-on response of naphthalimide based probes for selective thiophenol sensing, RSC Adv., 4 (2014) 59579-59586.

[37] Y.N. Shen, L. Lin, H.Y. Qiu, W.Y. Zou, Y. Qian, H.L. Zhu, The design, synthesis, in vitro biological evaluation and molecular modeling of novel benzenesulfonate derivatives bearing chalcone moieties as potent anti- microtubulin polymerization agents, RSC Adv., 5 (2015) 23767-23777.
[38] I. Kaabi, L. Sibous, T. Douadi, S. Chafaa, X-ray structure of a new ligand: Di[(4-phenylimino) 4-diethyl salicylaldehyde] ether and electrochemical study of its copper (II) and cobalt (II) complexes, J. Mol. Struct., 1084 (2015) 216-222.
[39] K.M. Hutchins, S. Dutta, B.P. Loren, L.R. MacGillivray, Co-Crystals of a Salicylideneaniline: Photochromism Involving Planar Dihedral Angles, Chem. Mater., 26 (2014) 3042-3044.
[40] J. Pitchaimani, M.R.C. Raja, S. Sujatha, S.K. Mahapatra, D. Moon, S.P. Anthony, V. Madhu, Arene ruthenium(II) complexes with chalcone, aminoantipyrine and aminopyrimidine based ligands: synthesis, structure and preliminary evaluation of anti-leukemia activity, RSC Adv., 6 (2016) 90982-90992.
[41] I. Cassells, T. Stringer, A.T. Hutton, S. Prince, G.S. Smith, Impact of various lipophilic substituents on ruthenium(II), rhodium(III) and iridium(III) salicylaldimine-based complexes: synthesis, in vitro cytotoxicity studies and DNA interactions, J. Biol. Inorg. Chem., 23 (2018) 763-774.
[42] W.G. Jia, Z.B. Wang, X.T. Zhi, J.Q. Han, Y. Sun, Syntheses, characterization and catalytic activities of half-sandwich ruthenium complexes with naphthalene-based Schiff base ligands, J. Coord. Chem., 70 (2017) 848-858.
[43] W. Nkoana, D. Nyoni, P. Chellan, T. Stringer, D. Taylor, P.J. Smith, A.T. Hutton, G.S. Smith, Heterometallic half-sandwich complexes containing a ferrocenyl motif: Synthesis, molecular structure, electrochemistry and antiplasmodial evaluation, J. Organomet. Chem., 752 (2014) 67-75.
[44] W.G. Jia, H. Zhang, T. Zhang, D. Xie, S. Ling, E.H. Sheng, Half-Sandwich Ruthenium Complexes with Schiff-Base Ligands: Syntheses, Characterization, and Catalytic Activities for the Reduction of Nitroarenes, Organometallics, 35 (2016) 503-512.
[45] S. Acharya, M. Maji, Ruturaj, K. Purkait, A. Gupta, A. Mukherjee, Synthesis, Structure, Stability, and Inhibition of Tubulin Polymerization by Ru-II-p-Cymene Complexes of Trimethoxyaniline-Based Schiff Bases, Inorg. Chem., 58 (2019) 9213-9224.
[46] A. Inan, A.B. Sunbul, M. Ikiz, S.E. Tayhan, S. Bilgin, M. Elmastas, K. Sayin, G. Ceyhan, M. Kose, E. Ispir, Half-sandwich Ruthenium(II) arene complexes bearing the azo-azomethine ligands: Electrochemical, computational, antiproliferative and antioxidant properties, J. Organomet. Chem., 870 (2018) 76-89.
[47] L. Biancalana, I. Abdalghani, F. Chiellini, S. Zacchini, G. Pampaloni, M. Crucianelli, F. Marchetti, Ruthenium Arene Complexes with -Aminoacidato Ligands: New Insights into Transfer Hydrogenation Reactions and Cytotoxic Behaviour, Eur. J. Inorg. Chem., (2018) 3041-3057.
[48] N. Mohan, M.K.M. Subarkhan, R. Ramesh, Synthesis, antiproliferative activity and apoptosis-promoting effects of arene ruthenium(II) complexes with N, O chelating ligands, J. Organomet. Chem., 859 (2018) 124-131.
[49] A. Inan, M. Ikiz, S.E. Tayhan, S. Bilgin, N. Genc, K. Sayin, G. Ceyhan, M. Kose, A. Dag, E. Ispir, Antiproliferative, antioxidant, computational and electrochemical studies of new azo-containing Schiff base ruthenium(II) complexes, New J. Chem., 42 (2018) 2952-2963.
[50] A.C. Matsheku, M.Y.H. Chen, S. Jordaan, S. Prince, G.S. Smith, B.C.E. Makhubela, Acridine-containing Ru-II, Os-II, Rh-III and Ir-III Half-Sandwich Complexes: Synthesis, Structure and Antiproliferative Activity, Appl. Organomet. Chem., 31 (2017).
[51] E. Ekengard, L. Glans, I. Cassells, T. Fogeron, P. Govender, T. Stringer, P. Chellan, G.C. Lisensky, W.H. Hersh, I. Doverbratt, S. Lidin, C. de Kock, P.J. Smith, G.S. Smith, E. Nordlander, Antimalarial activity of ruthenium(II) and osmium(II) arene complexes with mono- and bidentate chloroquine analogue ligands, Dalton Trans., 44 (2015) 19314-19329.
[52] K. Ghebreyessus, A. Peralta, M. Katdare, K. Prabhakaran, S. Paranawithana, Ruthenium(II)-arene complexes with naphthalimide-tagged N,O- and N,N-chelating ligands: Synthesis and biological evaluation, Inorg. Chim. Acta, 434 (2015) 239-251.

[53] A.R. Burgoyne, B.C.E. Makhubela, M. Meyer, G.S. Smith, Trinuclear Half-Sandwich Ru-II, Rh-III and Ir-III Polyester Organometallic Complexes: Synthesis and in vitro Evaluation as Antitumor Agents, Eur. J. Inorg. Chem., (2015) 1433-1444.
[54] B.C.E. Makhubela, M. Meyer, G.S. Smith, Evaluation of trimetallic Ru(II)- and Os(II)-Arene complexes as potential anticancer agents, J. Organomet. Chem., 772 (2014) 229-241.
[55] P. Govender, A.K. Renfrew, C.M. Clavel, P.J. Dyson, B. Therrien, G.S. Smith, Antiproliferative activity of chelating N,O- and N,N-ruthenium(ii) arene functionalised poly(propyleneimine) dendrimer scaffolds, Dalton Trans., 40 (2011) 1158-1167.
[56] W.D.J. Tremlett, K.K.H. Tong, T.R. Steel, S. Movassaghi, M. Hanif, S.M.F. Jamieson, T. Sohnel, C.G. Hartinger, Hydroxyquinoline-derived anticancer organometallics: Introduction of amphiphilic PTA as an ancillary ligand increases their aqueous solubility, J. Inorg. Biochem., 199 (2019).
[57] A. Skoczynska, B. Pasternak, M. Malecka, U. Krajewska, M. Mirowski, A. Merecz-Sadowska, B.T. Karwowski, J. Kusz, E. Budzisz, The cytotoxic effect of Ru(II) complexes with 5-(2-hydroxyphenyl)-3-methyl-1-(2-pyridyl)-1H-pyrazole-4-carboxylic acid methyl ester: Synthesis, X-ray structure and DNA damage potential, Polyhedron, 169 (2019) 228-238.
[58] G.S. Yellol, J.G. Yellol, V.B. Kenche, X.M. Liu, K.J. Barnham, A. Donaire, C. Janiak, J. Ruiz, Synthesis of 2-Pyridyl-benzimidazole Iridium(III), Ruthenium(II), and Platinum(II) Complexes. Study of the Activity as Inhibitors of Amyloid-beta Aggregation and Neurotoxicity Evaluation, Inorg. Chem., 54 (2015) 470-475.
[59] A. Ashraf, F. Aman, S. Movassaghi, A. Zafar, M. Kubanik, W.A. Siddiqui, J. Reynisson, T. Sohnel, S.M.F. Jamieson, M. Hanif, C.G. Hartinger, Structural Modifications of the Antiinflammatory Oxicam Scaffold and Preparation of Anticancer Organometallic Compounds, Organometallics, 38 (2019) 361-374.
[60] R. Pettinari, F. Marchetti, C. Di Nicola, C. Pettinari, A. Galindo, R. Petrelli, L. Cappellacci, M. Cuccioloni, L. Bonfili, A.M. Eleuteri, M.F.C.G. da Silva, A.J.L. Pombeiro, Ligand Design for N,O- or N,N-Pyrazolone-Based Hydrazones Ruthenium(II)-Arene Complexes and Investigation of Their Anticancer Activity, Inorg. Chem., 57 (2018) 14123-14133.

In this work, a new N,O-type ligand containing a sulfonate ester group and its heteroleptic Ru(II) complex have been synthesized and experimentally and theoretically characterized. The synthesized compounds exhibited good cytotoxicity towards human neuroblastoma cancer cells and antibacterial effects towards 16 bacterial strains.

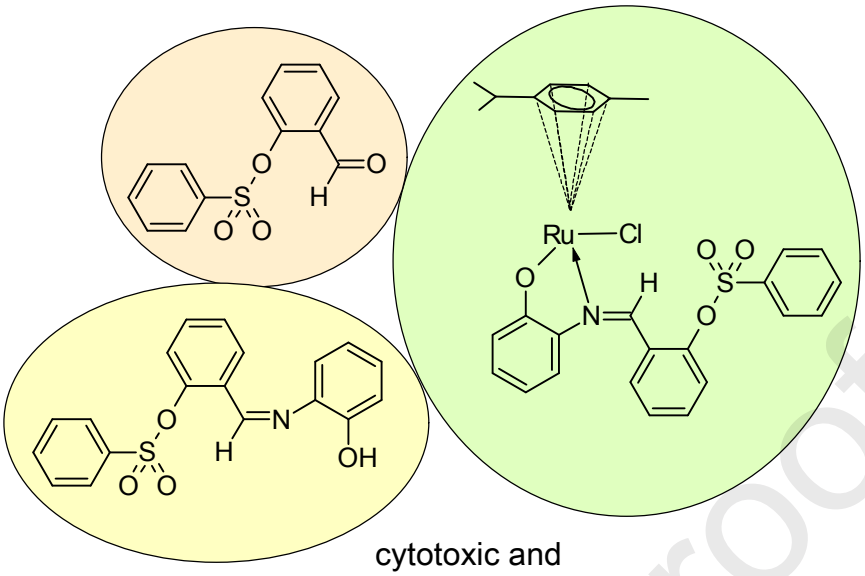

cytotoxic and
antibacterial effect